Microwave-energy coupling in a nitrogen-breakdown plasma

C. L. Yee,[a] A. W. Ali, and W. M. Bollen[a]
Naval Research Laboratory, Washington, D.C. 20375

(Received 20 September 1982; accepted for publication 22 October 1982)

Computer simulations of microwave coupling to a nitrogen-breakdown plasma have been performed at 25 Torr. Nonhydrodynamic ionization fronts are observed to propagate toward the radiation source under a variety of circumstances. Free-nitrogen-breakdown simulations in a spherical system show the propagation velocity of the breakdown wave can be as high as 5×10^6 cm/sec. An elementary theory is used for estimating the speed of the breakdown wave in one dimension. The results are in reasonable agreement with breakdown experiments.

PACS numbers: 52.40.Db, 52.50.Dg, 52.80.Pi

I. INTRODUCTION

The pulsed breakdown in air and other gaseous elements has been studied extensively[1] with emphasis on the threshold power for breakdown and its dependence on the gas pressure and radiation wavelength. The hydrodynamic effects were first considered by Lin and Theofilos.[2] Their calculation of the gas heating showed that both high-field intensity above the breakdown intensity and increasing molecular density discouraged energy deposition in air. Though the preliminary experimental results confirmed the general features of the simple theory, the observed pressure waves were stronger than predicted. Scharfman *et al.*[3] have observed that a breakdown plasma prevents the transmission of microwave energy to points beyond the plasma. Experiments[4] recently performed at the Naval Research Laboratory (NRL) showed that the microwaves are rapidly decoupled from a target or plasma surface. This rapid decoupling of the microwaves would limit the amount of energy that can be deposited into the gas. Computer simulations of the NRL experiments have been performed at a pressure of 25 Torr in nitrogen. Throughout this work, we have used the MINI code developed at NRL to help in understanding the basic interaction processes in the experiments.

II. THE MICROWAVE NITROGEN INTERACTION CODE (MINI)

The microwave nitrogen interaction code (MINI) used in our studies is a one-dimensional multispecies, multitemperature, hydrodynamic, nitrogen chemistry and wave optics code. The species followed dynamically were N_2, $N_2^+(X)$, $N_2^+(B)$, N_4^+, N, $N(^2D)$, $N_2(A\,^3\Sigma)$, $N_2(B\,^3\pi)$, $N_2(C^3\pi)$, and the electron density (n_e). The model calculates the electron (T_e), vibrational (T_v), and gas (T_g) temperatures, and is space and time dependent with microwave absorption and reflection considered in the wave-optics mode. The detail of the chemistry and the wave-optics aspect of the code are described elsewhere[5] and will not be repeated here. The electrons are described hydrodynamically by the equations

$$\partial_t(n_e) + \partial_y(n_e u_e) = C_e, \tag{1}$$

$$u_e = u_m - \mu_e E - D_e\partial_y(\ln n_e) - D_e\partial_y(\ln T_e), \tag{2}$$

$$\partial_t(\epsilon_e) + \partial_y\{\epsilon_e \mathbf{u}_e + p_e\mathbf{u}_e + \mathbf{Q}_e\} = \mathbf{R}_e\cdot\mathbf{u}_e + \mathbf{J}_e\cdot\mathbf{E} + E_e$$

$$\epsilon_e = \frac{3}{2}n_eT_e + \frac{1}{2}m_en_eu_e^2, \tag{3}$$

where $p_e = n_eT_e$ is the electron pressure, $j_e = -en_eu_e$ is the electron current density, $R_e = -m_en_e\nu_c(u_e - u_m)$ is the electron momentum transfer rate, $\mu_e = e/m_e\nu_c$ is the electron mobility, and $D_e = T_e/m_e\nu_c$ is the electron diffusion coefficient. The electron momentum transfer frequency is ν_c, and m_e is the mass of the electron. The electron energy flux $Q_e = -\kappa_e\partial/\partial_y T_e$, where the electron thermal conductivity is $\kappa_e = \beta n_eT_e/m_e\nu_c$, and β is a constant. The terms on the right-hand side of the energy equation represent energy lost due to heat flow, work due to momentum transfer, joule heating and heating due to elastic, inelastic, and chemical processes. The term C_e represents sources and sinks terms for the electron due to ionization, recombination, and attachment. The E_e term in the electron-energy equation includes energy losses due to vibrational and electronic excitation of molecular nitrogen. The C_e and E_e terms are discussed more fully in Ref. 5.

The continuity equation for each of the heavy particle species is

$$\partial_t(n_i) + \partial_y(n_iu_i) = C_i. \tag{4}$$

The momentum equation for the heavy particles is

$$\partial_t(\rho u) + \partial_y\{\rho u^2 + P_H - \left(\frac{4}{3}\mu + \mu_B\right)\partial_y u\} = \rho^+E - R_e, \tag{5}$$

where $P_H = \Sigma n_iT_g$ is the heavy particle pressure, $\rho = \Sigma m_i n_i$ is the mass density, $\rho^+ = \Sigma Z_i e n_i$ is the positive charge density, and $\mu(\mu_B)$ is the kinematic (bulk) viscosity coefficients. The transport coefficients for the viscosity and thermal conductivity are taken from Ref. 6. The heavy-particle energy equation is

$$\partial_t(\epsilon_H) + \partial_y\{\epsilon_H u + \{P_H - (\frac{4}{3}\mu + \mu_B)\partial_y\}u + Q_H\} \tag{6}$$
$$= n_m\tau_v^{-1}\{\epsilon_v(T_v) - \epsilon_v(T_g)\} - j_eE - R_eu_e + E_H$$

$$\epsilon_H = \sum_i c_in_iT_g + \frac{1}{2}\rho u^2,$$

where ϵ_H is the total energy density, c_i is the translation-rotational specific heat, $\epsilon_v(T_v) = \epsilon\{\exp(\epsilon/T_v) - 1\}^{-1}$ is the

[a] Mission Research Corporation, Alexandria, VA 22304.

 0021-8979/83/031278-06$02.40

average vibrational energy per molecule,[7] $\epsilon \simeq 0.3$ eV is the quantum of vibrational energy for nitrogen, τ_v is the characteristic time for vibrational relaxation,[8] and E_H is the heating terms due to chemical, elastic, and inelastic processes. Again a more detailed discussion of E_H can be found in Ref. 5. The heavy-particle energy flux is $Q_H = -\kappa_H \partial/\partial_y T_g$, and κ_H is the thermal conductivity of the gas, including translational and rotational contribution.[9] The mass-average-velocity of the heavy particles is

$$u = \frac{1}{\rho} \sum_i m_i n_i u_i \simeq u_m .$$

The vibrational energy equation may be written approximately as

$$\partial_t \{n_m \epsilon_v(T_v)\} + \partial_y \{n_m \epsilon_v(T_v) u_m + Q_v\}$$
$$= -\frac{n_m}{\tau_v} \{\epsilon_v(T_v) - \epsilon_v(T_g)\} + E_v,$$

where $Q_v = -\kappa_v \partial_y T_v$ is the vibrational energy flux and κ_v is the vibrational conductivity. The vibrational temperature can be calculated assuming that the nitrogen molecule is a harmonic oscillator and that the vibrational levels have a Boltzman distribution. Hence, the vibrational energy source term due to electron impact is[10]

$$E_v = \epsilon n_m n_e \{1 - \exp(-\epsilon/T_v)]$$
$$\Sigma_{v=1}^{8} v X_v \{1 - \exp\{\epsilon v (T_v - T_e)/T_v T_e\}\}, \quad (7)$$

where X_v is the excitation rate coefficient[10] for the vth vibrational level obtained from the experimentally measured cross sections.[11]

The dc portion of the electric field and the diffusion velocities are determined by demanding the total current

$$\mathbf{J}_T = \mathbf{J}_e + \sum_i \mathbf{J}_i = 0, \quad (8)$$

where $J_i = Z_i e n_i u_i$ is the current density of the ith ion species. In steady state, each of the ion species satisfies an equation:

$$\mathbf{u}_i = \mathbf{u}_m + \mu_i \mathbf{E} - D_i \partial_y (\ln n_i) - D_i \partial_y (\ln T_g), \quad (9)$$

where the ion diffusion coefficient and mobility are related to the collision frequency ν_i by $D_i = T_g/M_i \nu_i$ and $\mu_i = Z_i e/m_i \nu_i$. The mass of the ith ion species is m_i. Summing Eq. (9) for all ion species and using Eq. (8) gives an equation for the ambipolar electric field. Once the ambipolar field is found, Eqs. (9) and (2) are used to solve for the flow velocities of the ions and the electron.

The Eulerian difference equations of Eqs. (1)–(7) are solved using the algorithm of Rubin and Burstein.[12] The scheme is simple, second order in accuracy, and is relatively stable while centering the dissipation terms. The hydrodynamics are determined from the updated values of the chemistry. Hence, the hydrodynamics are considered as a small correction to the chemistry.

II. CASCADE IONIZATION OF NITROGEN BY A MICROWAVE PULSE

Microwave gas breakdown begins when a small number of priming electrons acquire sufficient energy from the electric field to ionize the gas. The priming electrons gain energy when the oscillatory energy of the electrons in the electric field is randomized by collisions into thermal energy. Once an electron has an energy in excess of the ionization energy of the gas, the electron can easily ionize the gas, resulting in the generation of two low-energy electrons. The electron avalanche can be described by

$$n_e(t) = n_e(0) \exp(t/\tau_B), \quad (10)$$

where $n_e(t)$ is the electron density at time t, and τ_B is the breakdown time. Physically, τ_B is the time required for an electron to gain the energy needed to ionize the gas.[13] Figure 1 shows the breakdown time τ_B (sec) and the electron temperature T_e(eV) for conditions typical of microwave breakdown of N_2. A high radiation field would promote the electron avalanche by increasing the energy imparted to the electron per collision with the molecule. A high molecular density, however, requires higher intensities for the avalance breakdown. At moderate pressures above 25 Torr, the dominant energy loss mechanism for the electrons is the excitation of the electronic and vibrational modes of the gas. The root-mean-square electric field to density ratio E/n_m (V cm^2) does not uniquely define the absorbed energy for an ac electric field. The striped region in Fig. 1 is bounded by the constant intensity line (I) and the constant pressure line (P). The rapid variation in τ_B with increasing intensity allows a breakdown threshold, I_B, to be assigned at the onset of breakdown. The ability to couple microwave energy to a breakdown gas depends sensitively on the breakdown time, τ_B, and the electron density.

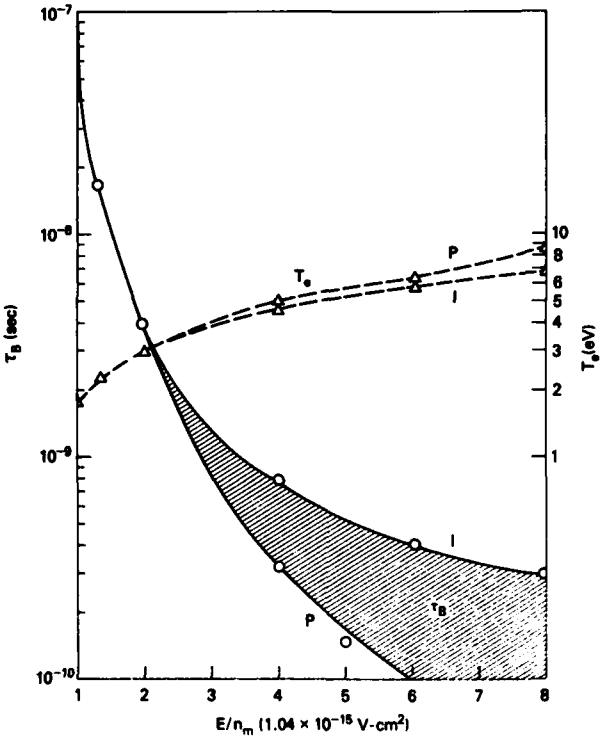

FIG. 1. The breakdown time and the electron temperature vs the rms electric field to density ratio E/n_m.

The efficiency of converting microwave energy to the translational energy of the gas can be enhanced by coupling the microwaves to a preformed plasma. Plasma maintenance of the preformed plasma by microwaves allows the microwave deposition to be localized while maintaining a high electron density. In short-pulse breakdown experiments, with pulse lengths $\tau_p < 1$ μsec, a high electron density is a necessary condition for rapid heating of the gas. Plasma maintenance requires the breakdown time $\tau_B > \tau_p$ when $n_e(0) \gg 1$. If the local electric field is not carefully matched to the instantaneous plasma conditions, the gas heating will be self-limited by the formation of a nonhydrodynamic ionization front. Gas breakdown off a reflecting surface without a preformed plasma will not result in a local deposition of the microwave energy. Since the microwave deposition is determined self-consistently with the electron density profile, the resulting plasma density cannot rapidly heat the gas in the short-pulse experiments.

A. Gas breakdown near a reflecting surface

A plane wave incident normal to a reflecting surface requires less power for gas breakdown. The constructive interference of the incident and reflected microwave results in the characteristic standing wave pattern for the electric field and a factor of 4 increase in the field intensity. If the intensity is above the breakdown threshold, breakdown of the gas occurs intantaneously at the peak nodes of the electric field. As the electron density rises, these "pancakes" of electrons begin to attenuate the radiation. Pancakes closest to the reflecting surface rise more rapidly early in the pulse (Fig. 2). As the electron density continues to rise, attenuation of the microwave causes the pancakes closest to the surface to fall in density below that of pancakes far from the surface. Shorter systems with fewer pancakes decouple more rapidly than longer systems. However, the total absorbed energy remains essentially constant, independent of the system size for a fixed pressure and pulse length.[14]

The finite-length simulations represent the planar region near the surface of a focused microwave system where the distance from the surface is less than the radius of the spotsize. Figure 2 shows two similar simulations with $I = 6.25\ \mathrm{kW/cm^2}$ for a one-and-a-half and three wavelength system without hydrodynamic effects. The plasma absorbs approximately 20% of the total microwave energy with an asymptotic absorption efficiency of 80%. The absorption is regulated by the electron density. Shorter systems have a much higher electron density than larger systems and can more readily heat the gas in the short-pulse experiments. The gas is not expected to be heated more than the observed 4% above the ambient temperature in a weakly focused system. The absorbed energy is distributed over a larger number of pancakes with a very low electron density. As will be discussed later, the low electron density of Fig. 2 results in a long heating time for the gas of $\tau_g \simeq 6.5\,\mu$ sec, where $\tau_g \equiv T_g (dT_g/dt)^{-1}$. The time required to heat the gas to an appreciable temperature in a weakly focused system would require pulse lengths of $\tau_p \gg 6.5\,\mu$ sec. However, even for long pulses, a significant heating of the gas is never realized. Later in the pulse, the pancakes furthest away from the reflecting surface continue to rise in density. Ultimately, a single pancake will have sufficient density to reflect the radiation. This pancake

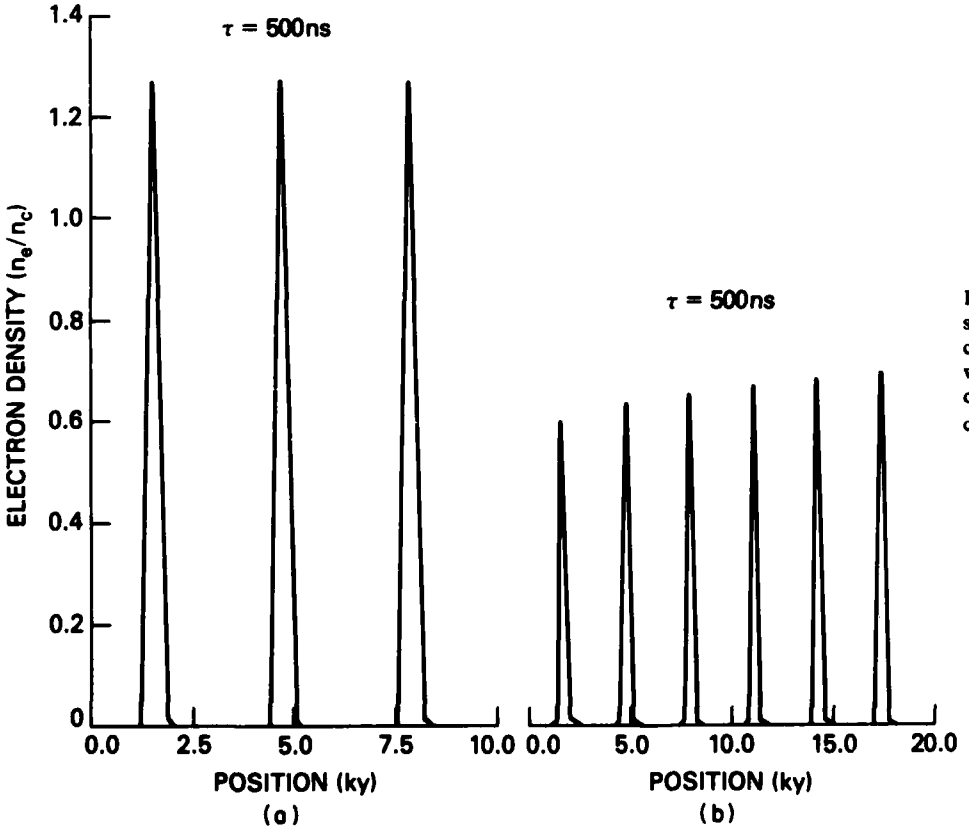

FIG. 2. Gas breakdown near a reflecting surface showing the electron-density pancakes for (a) one-and-a-half and (b) three wavelengths planar system. The critical density is $n_c = 1.5\times10^{13}$ and $k = 7.33\ \mathrm{cm^{-1}}$.

acts as a secondary reflecting surface and decouples the radiation from the primary metallic surface. Gas-breakdown experiments[4] using a reflecting surface show this behavior. Similarly, free-nitrogen-breakdown simulations without a surface, using a focused system, also show that the radiation is decoupled from the initial breakdown site.

B. Maintenance of a preformed plasma by microwaves

Microwave coupling to a preionized plasma near a metallic surface show some general characteristics. Though the plasma absorbs the microwave energy, the absorption cannot be localized. A traveling ionization front is observed to proceed toward the radiation source. Figure 3 shows the time history of the ionization front in the strong mismatch case $I \gg I_B$ and $\tau_p > \tau_C$. The critical time τ_C is the time required for the electron avalanche to reach the critical density $n_c \equiv \omega^2 m_e / 4\pi e^2 \simeq 10^{13}/\lambda^2$(cm), where λ is the wavelength of the incident radiation. In this simulation $I = 12.5$ kW/cm$^2 \gg I_B = 3$ kW/cm^2, $\tau_p = 0.5\,\mu$sec, $\tau_C = 0.16\,\mu$sec, and all hydrodynamic effects are suppressed. The initial electron density (preionized plasma) was initialized with a symmetric profile with a peak density of 0.1 n_c and full width half-maximum of 0.1 λ. In Fig. 3, the peak density is determined by Eq. (10). However, the breakdown time τ_B is a complicated function of the incident and reflected microwaves. It is clear that the small reflectivity ($R < 10\%$) is important in determining the propagation speed since, as Fig. 3 shows, the separation distance between peaks is $\lambda/4$. The ionization front proceeds toward the source at a characteristic speed $D(t) = \lambda/4\tau_C(t)$. The maximum density is decreasing with time while the total absorption continues to increase with time. The asymptotic efficiency is approximately 95%. The movement of the ionization front limits the time the gas-plasma system samples the radiation field. The sampling time τ_S is determined by $\alpha(\text{cm}) = \int_0^{\tau_S} D(t)\,dt \simeq D(0)\tau_S$, where $D(0) = \lambda/4\tau_C(0) \simeq 1.6 \times 10^6$ cm/sec is the early-breakdown speed. Estimating the absorption length as $\alpha(\text{cm}) \simeq \lambda/2\pi$ gives a sampling time of $\tau_S \simeq \tau_C$. In the pressure regime $P > 25$ Torr, the gas is primarly heated through the quenching of the electronic states by molecular and atomic nitrogen. The fractional change in the gas temperature is $\epsilon_g \equiv (\Delta T_g/T_g)_{\max} = \tau_S \Sigma_{\alpha\beta} Q_{\alpha\beta} n_\alpha n_\beta \epsilon_\alpha / c_v n_m T_g$, where $Q_{\alpha\beta}$ is the quenching rate of the N_2 triplet state n_α by n_β. The specific heat of nitrogen is c_v, and ϵ_α is the energy level of the n_α state. As an example, the $N_2(C^3\pi)$ state is quenched by N_2 with a rate coefficient[15] of 1.2×10^{-11} cm^3/sec. The fractional change in the gas temperature ϵ_g is approximately 21% from the ambient temperature.

The region of the maximum gas heating is at the initial breakdown site ($\sim\lambda/4$ from the surface). The electric field is less than 1% of the incident time-average electric field at the maximum gas temperature [Fig. 4(a)]. The plasma absorbs approximately 70% of the incident microwave energy and has an electron temperature of less than 2.5 eV [Fig. 4(b)]. Maximum gas heating requires the sampling time and the electron temperature to be as large as possible without decoupling the system. A high electron temperature populates the electronic states which are rapidly quenched to heat the gas. Approximately 4% and 40% of the incident energy goes into heating the gas and exciting the vibrational states. A similar simulation with the peak power reduced to $I = 6.25$ kW/cm^2 shows no movement of the initial ionization region while increasing the fractional change in the gas temperature to 27%. Further irradiance would increase the gas temperature.

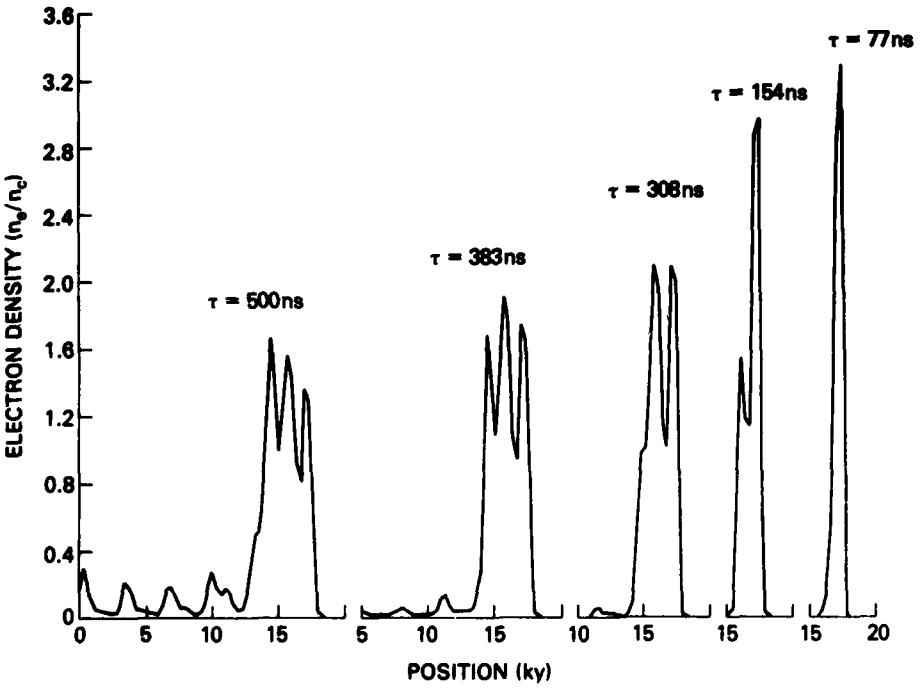

FIG. 3. Time history of the ionization front in a planar system showing the wave motion toward the radiation source. The microwaves are incident from the left onto a preionized plasma near a reflecting surface on the right boundary. The normalization parameters are the same as in Fig. 2.

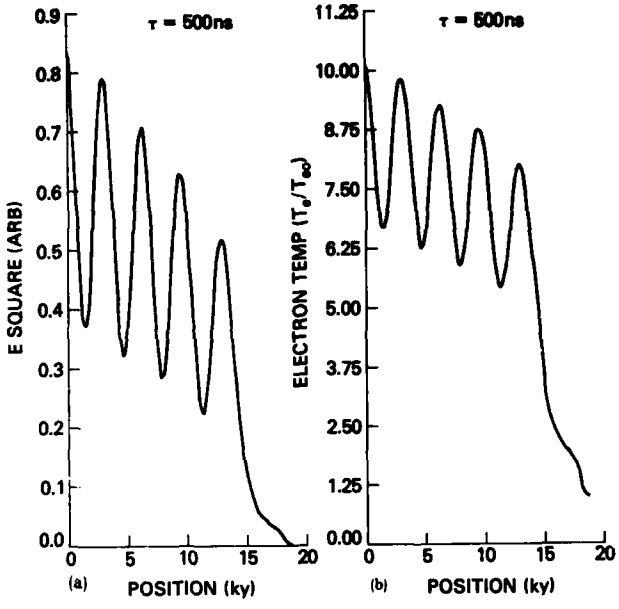

FIG. 4. (a) The time-averaged electric field square and (b) the electron temperature vs position. The normalization parameters are: $T_{e0} = 0.25$ eV, $k = 7.33\ \text{cm}^{-1}$, and the arbitrary units of $\langle E^2 \rangle = 1$ correspond to an average intensity of $9.4\ \text{kW/cm}^2$.

C. Gas breakdown in a focused microwave system

Simulations of a focused microwave system were also performed. If the field intensity in a focused system greatly exceeds the breakdown threshold at the focal spot, a breakdown wave propagates toward the source.[16] The motion of the microwave plasma absorbing layer is not a simple-breakdown wave, since the reflected microwave is important in determining the propagation speed. Figure 5 shows the time history of the electron density profile during the course of a $\tau_p = 0.5$-μsec pulse in a focused system. The spherical wave equation is solved for the electric field to model the convergence of the field. The peak incident field is $I = 10\ \text{kW/cm}^2$ with a system aspect ratio of 2.5. The average power at focus is $31.25\ \text{kW/cm}^2$, and all hydrodynamic effects are suppressed. The very rapid early-time speed of the absorbing wave, $D \simeq 5 \times 10^6$ cm/sec, gives a sampling time of $\tau_S \simeq 1.7 \times 10^{-8}$ sec. However, the gas continues to be heated after the passage of the field by the de-excitation of the electronic states. The miximum gas and vibrational temperature are $\epsilon_g \simeq 10\%$ and $\epsilon_v \simeq 260\%$, respectively. The quarter-wavelength fine structure in the density profile shows the effected light. The time-average reflection and absorption coefficient are 19% and 68%, respectively. A snapshot of the electric field and electron temperature (Fig. 6) shows the lack of field penetration ($\alpha \simeq 0.1\lambda$) and the cold plasma temperature, $T_e < 3.3$ eV. The gas and vibration temperatures again are reduced when hydrodynamic effects are included in the simulations. The gas is expected to be heated, at most, to 10% of the initial value during the course of a 0.5-μsec pulse.

The propagation velocity of the breakdown wave in a focused microwave system can be calculated. Simulations show the absorption is localized at the head of the breakdown wave. The reflection coefficient is relatively constant after the initial breakdown ($t > \tau_C$). The breakdown time τ_B is inversely proportional to the light flux $1/\tau_B \propto (1 + 2\,\text{Re}\,\xi + \xi^2)I$, where the reflection coefficient is ξ^2. The intensity in a conically focused system can be written as

$$I(X,t) \propto \frac{(1 + 2\,\text{Re}\,\xi + \xi^2)}{r^2} \times \phi(t),$$

where $\phi(t)$ is a form function characterizing the pulse. The radius of the radiation channel at position X on the channel axis is $r = r_0 + X \tan\theta$. The minimum radius of the waist at the focal point is r_0, and θ is the half-angle of the radiation column. Following Raizer,[16] the propagation velocity of the

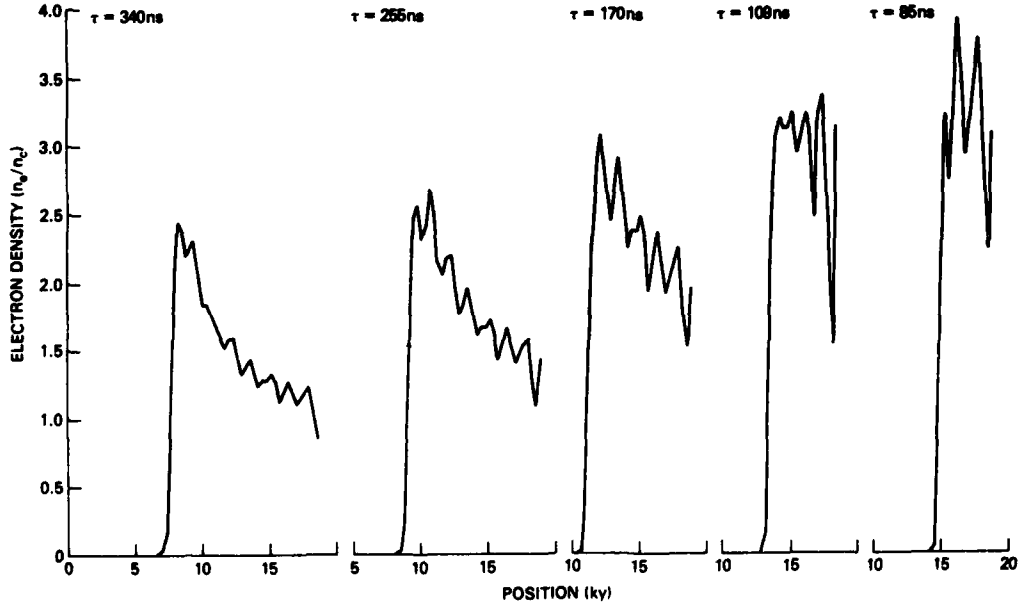

FIG. 5. Time history of the ionization front in a spherical system. The microwaves are incident from the left boundary with an intensity of $5\ \text{kW/cm}^2$. The focused average power is $31.25\ \text{kW/cm}^2$ at the right-side boundary.

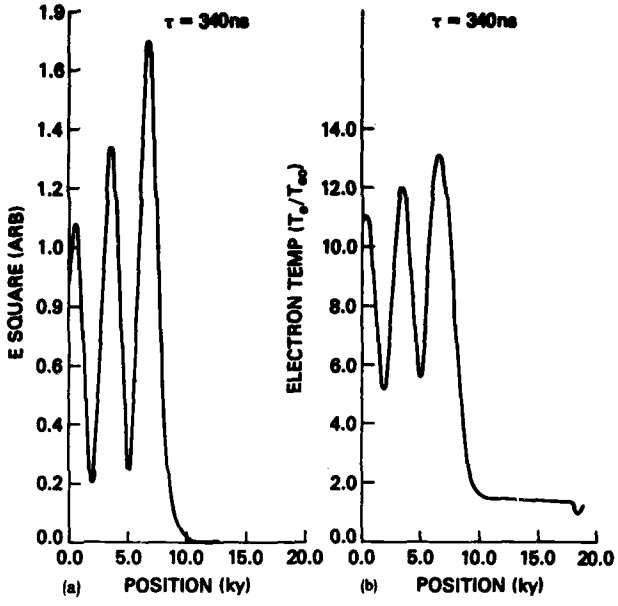

FIG. 6. (a) The time-averaged electric field square and (b) the electron temperature vs position for the simulation of Fig. 5. The normalization parameters are the same as in Fig. 4.

breakdown wave is approximately $D = r_0/\tau_C \tan\theta$. Under the assumptions made, the velocity D would be an upper bound on the propagation velocity of the breakdown wave.

IV. SIMULATION OF THE NRL EXPERIMENTS

We compare the simulation results with the NRL experiment. The NRL 35-GHz 112-kW focused gyro[illegible]ystem gives an average power at the focal spot of 33 kW/cm^2. The polarization of the microwave is such that the electric field is perpendicular to the plasma gradient (S polarization). The average aspect ratio of the experiment gives an equivalent simulation aspect ratio of 2.5. The free-nitrogen breakdown experiments were performed at 25 Torr with a 100 pps repetition rate at $\tau_p = 1.5\,\mu$sec. The minimum radius of the waist at the focal spot is $r_0 = 0.75$ cm, and the half-angle of the radiation column satisfies $\tan\theta = 0.35$. Experimentally, framing camera data (Fig. 7) gives a propagation velocity of $D \simeq 4.6\times10^6$ cm/sec. The width of the absorbing wave is approximately 1.2 cm. The measured absolute intensity of the second positive band, N_2 $2P$ (0-0) at 3371 Å, is 1.4×10^{21} eV/cm^2 sec. The calculated spatial width of the 3371-Å light emission is 0.8 cm, with a peak intensity of 1.8×10^{21} eV/cm^2 sec. As mentioned previously, the calculated speed of the breakdown wave is 5×10^6 cm/sec. Experimentally, the inferred breakdown time is $\tau_B \simeq 2.5\times10^{-8}$ sec or $\tau_C \simeq 7.4\times10^{-7}$ sec. This is to be compared to the calculated breakdown time early in the pulse, $\tau_B \simeq 4.5\times10^{-9}$ sec, and late in the pulse, $\tau_B \simeq 6\times10^{-8}$ sec. The simulation results are felt to be in reasonable agreement with the experiment.

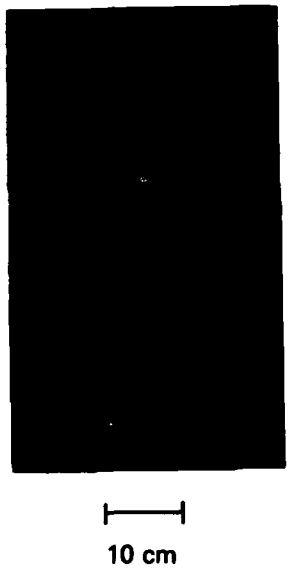

FIG. 7. Framing camera data showing the motion of the ionization front in a focused free-nitrogen-breakdown experiment. The top and bottom photographs were taken 0.2 and 0.1 μsec after the first observable breakdown.

V. CONCLUSION

In conclusion, computer simulation of microwave coupling to a weakly ionized gas plasma shows excellent absorption of the microwave energy. The electronic states of nitrogen excited by electron impact are rapidly quenched by molecular and atomic nitrogen to heat the gas at pressure above 25 Torr. However, high power irradiance can easily produce a non-hydrodynamic ionization front which can severely limit the heating of the gas. Microwave gas breakdown experiments with pulse lengths less than one microsecond are expected to show only a slight heating of the gas.

[1] A. D. MacDonald, *Microwave Breakdown in Gases* (Wiley, New York, 1966).
[2] S. C. Lin and G. P. Theofiles, Phys. Fluids **6**, 1369 (1963).
[3] W. E. Scharfman, W. C. Taylor, and T. Murita, IEEE Trans. Antennas Propag. **12**, 709 (1964).
[4] W. M. Bollen, C. L. Yee, A. W. Ali, M. J. Nagurney, and M. E. Read, "High Power Microwave Energy Coupling to Nitrogen During Breakdown," NRL Memo Report 4865, 1982.
[5] C. L. Yee and A. W. Ali, "Microwave Energy Deposition, Breakdown, and Heating of Nitrogen and Air," NRL Memo Report 4617, 1981.
[6] R. B. Bird, *Transport Phenomena* (Wiley, New York, 1960).
[7] J. W. Rich, J. Appl. Phys. **42**, 2719 (1971).
[8] R. Millikan and D. White, J. Chem. Phys. **39**, 3209 (1963).
[9] H. C. Anderson, in *Kinetic Processes in Gases and Plasma*, edited by A. R. Hochstim (Academic, New York, 1969), Chaps. 2 and 3.
[10] A. W. Ali, "The Physics and Chemistry of Two NRL Codes for the Disturbed E and F Regions," NRL Memo Report 7578, 1973.
[11] G. J. Schulz, Phys. Rev. A **135**, 988 (1964); H. Ehrhardt and R. Willman, Z. Phys. **204**, 462 (1967); A. G. Engelhardt *et al.*, Phys. Rev. A **135**, 1566 (1964).
[12] E. L. Rubin and S. Z. Burstein, J. Comput. Phys. **2**, 178 (1967).
[13] Y. B. Zel'Dovich and Y. P. Raizer, Sov. Phys. JETP **20**, 772 (1965).
[14] Wee Woo and J. S. DeGroot, "Analysis and Computations of Microwave-atmospheric Interaction," Plasma Research Group Report, University of California at Davis, Department of Applied Science, 1981.
[15] P. Millet *et al.*, J. Chem. Phys. **58**, 5839 (1973).
[16] Y. P. Raizer, Sov. Phys. JETP **21**, 1009 (1965).